SUPPLEMENTAL FIGURE 1

Glutathione redox state of normal and SS RBCs. Measurement of total glutathione (GSH + GSSG) and GSSG alone (with calculation of GSH) in washed RBCs exposed to HX/XO. Glutathione-related parameters include half-cell reduction potential (E_{hc}) **(A, B)**, GSH_{Total} (GSH + GSSG) **(C, D)**, GSH alone **(E, F)**, and GSSG alone **(G, H)**. Data plotted as means ± SEM; (n = 5 – 8) * $p < 0.05$ normal vs sickle cell control; + $p < 0.05$ normal HX/XO exposed vs sickle cell HX/XO exposed.

SUPPLEMENTAL FIGURE 2

NADP/NADPH redox state of healthy control and SS RBCs. Measurement of $NADP_{Total}$ (free cytosolic NADP + NADPH) and NADPH alone (free cytosolic and protein bound) in washed RBC exposed to HX/XO. NADP/NADPH-related parameters include half cell reduction potential **(A, B)**, $NADP_{Total}$ ($NADP^+$ + free cytosolic NADPH) **(C, D)**, and NADPH alone (free cytosolic and protein bound) **(E, F)**. Data plotted as means ± SEM; (n = 5 – 8) * $p < 0.05$ normal control vs sickle cell control; + $p < 0.05$ normal HX/XO exposed vs sickle cell HX/XO exposed.

SUPPLEMENTAL FIGURE 3

Glutathione recycling in sickle cell RBCs is enhanced by channeling energy metabolism through the hexose monophosphate pathway. Measurement of total glutathione (GSH + GSSG) and GSSG alone (with calculation of GSH) in washed RBCs exposed to HX/XO or washed RBCs pre-incubated with KA (15µM final KA in 10% Hct RBC suspension, 37°C for 1 hour), prior to HX/XO exposure. Glutathione-related parameters include half cell reduction potential (*A, B*), GSH_{Total} (GSH + GSSG) (C*, D*), GSH alone (*E*, *F*), and GSSG alone (*G*, *H*). Data plotted as means ± SEM; (n = 3 – 5) * $p < 0.05$ sickle cell HX/XO exposed vs KA-treated sickle cell HX/XO exposed).

SUPPLEMENTAL FIGURE 4

Standardization of GAPDH activity assay and GAPDH inhibition by cdB3 peptide. A peptide limited to residues 1-12 of the band 3 NH_2 terminus was added at a final concentration (1-100μM) to GAPDH (24nM, final) from human erythrocytes (Sigma), in a total buffer volume of 1ml (10 mM imidazole acetate, 0.1 mM EDTA, 0.5 mM sodium arsenate, 1 mM sodium phosphate pH 7). Following 5 minute incubation, NAD^+ and G3P were added to start the reaction. Kinetic activity of GAPDH was measured monitoring absorbance at 340nm. **(A)** Standard curve of enzyme activity in the assay. **(B)** Inhibition of enzyme activity by the peptide.

SUPPLEMENTAL FIGURE 5

^{1}H NMR spectra indicating positional ^{13}C-enrichment in lactate isotopomers generated following HMP stimulation in normal and SSRBCs. As described in the text, RBCs were incubated with [2-^{13}C]-Glucose to generate pathway-specific lactate isotopomers (e.g. Q2→EMP, Q3→HMP). **(A-D)** Both normal and SSRBCs were studied (+/- MB to stimulate the HMP); representative spectra for each condition are shown (please refer to Figure 2 for description of raw signal processing and spectral deconvolution). For both RBC populations (normal and SS), we observed expected shifts in peak amplitude (↓Q2, ↑Q3) with MB stimulation; however, this shift is appreciably blunted in spectra obtained from MB-stimulated SSRBCs (please refer to Table 1, for HMP flux calculations). Note, while other small metabolites could contaminate the isotopomer pattern [most notably alanine (CH_3 ^{1}H signal expected at 1.46 ppm) and β-hydroxybutarate (CH_3 ^{1}H signal expected at 1.19 ppm)], we did not find this to be a problem.

SUPPLEMENTAL FIGURE 6

B3 Tyrosine phosphorylation is O_2-responsive and partially accounts for blunted EMP activation in deoxyRBCs. Washed RBCs were incubated in phosphatase inhibitor buffer; RBC O_2 content was manipulated and membrane proteins were extracted for immunoblotting and densitometry. **(A)** B3 pTyr densitometry is referenced to normal, oxygenated RBCs and is noted to increase with deoxygenation. In SSRBCs, pTyr density is increased at rest, and markedly so upon deoxygenation (25X level observed in normal, oxygenated RBCs). **(B)** We compared the influence of O_2 content and B3 phosphorylation (incubation with the phosphatase inhibitor O-vanadate) upon maximum HMP flux in normal RBCs (HMP was stimulated with methylene blue (MB)) [see text, Figure 2 and Table 1 for methodology and HMP flux calculations]). Maximum HMP flux was attenuated somewhat by O-vanadate incubation, but far less so than the attenuation observed by deoxygenation. This result suggests that while cdB3 phosphorylation displaces GAPDH to a degree (with consequent HMP constraint, see Figure 7 for full pathway schema); RBC O_2 content must also change to elicit the full HMP flux dampening observed in deoxygenated RBCs.

SUPPLEMENTAL FIGURE 7

Glucose utilization and lactate production in normal and SS RBCs. As described in the text, RBCs were incubated with glucose, the samples centrifuged and the supernatant collected. Glucose remaining and lactate accumulated (in the supernatant) was measured (by 1H NMR analysis and with either the Amplex Red Glucose Assay Kit, Inivtrogen or the EnzyFluo D-Lactate Assay Kit, BioAssay Systems, Hayward, CA). Correlation between NMR and **(A)** glucose measurements made by the Amplex Red glucose kit assay and **(B)** lactate measurements made by the EnzyFluo D-Lactate kit, demonstrating assay concordance. We determined glucose uptake over time for oxygenated normal and SS RBCs. (**C)** Glucose remaining in the extracellular media was plotted as a function of incubation time; the regression line slope (uptake rate) demonstrates a compensatory increase in glucose uptake by SS RBCs. **(D)** Lactate generation is plotted as a function of glucose uptake in oxygenated and deoxygenated normal RBCs (+/- MB; +/- KA); GPADH inhibition by KA significantly diminishes both glucose uptake and lactate production (distal EMP metabolism is required for lactate production, see Figure 7) .

SUPPLEMENTAL FIGURES

FIGURE 1

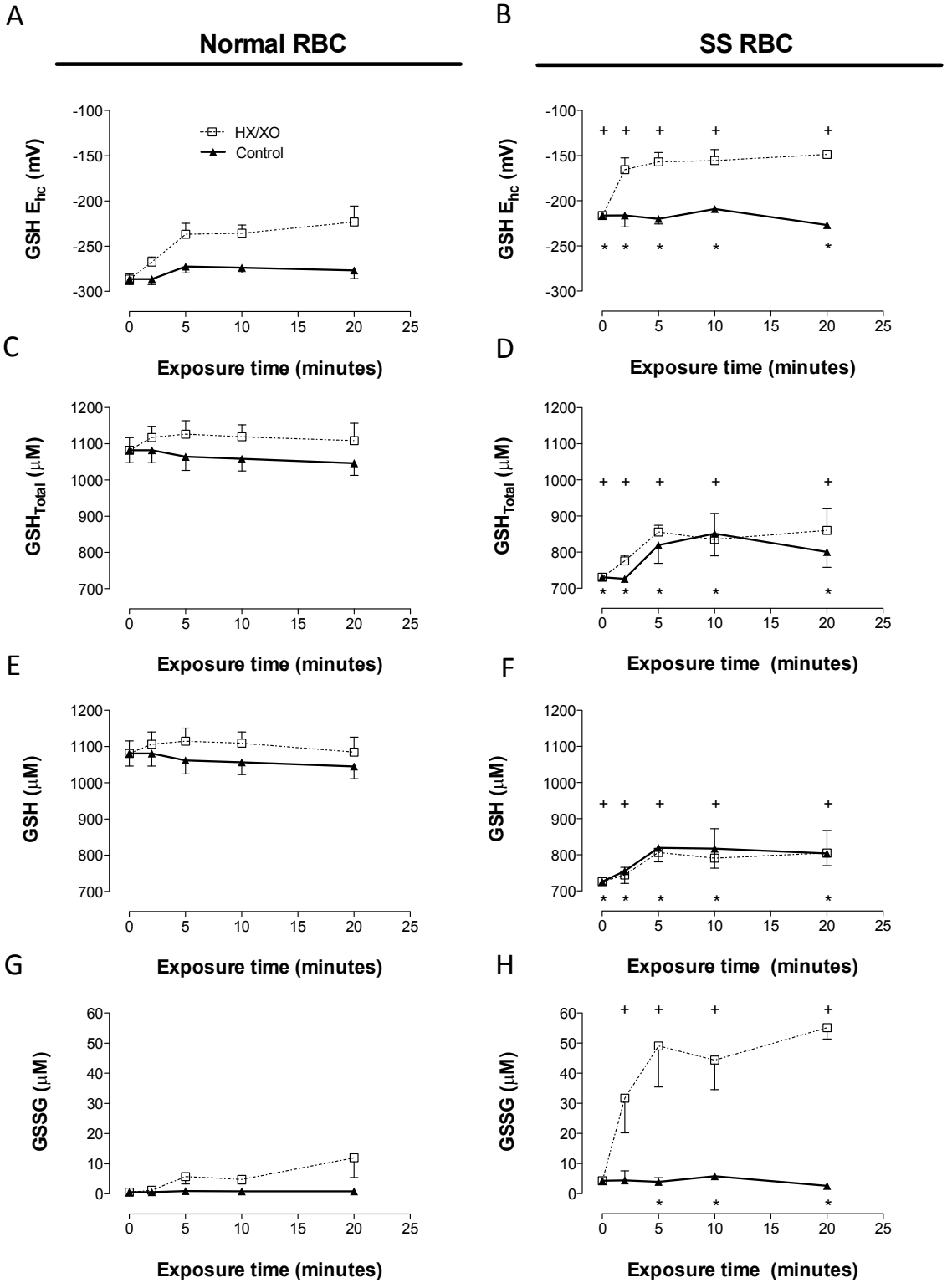

FIGURE 2

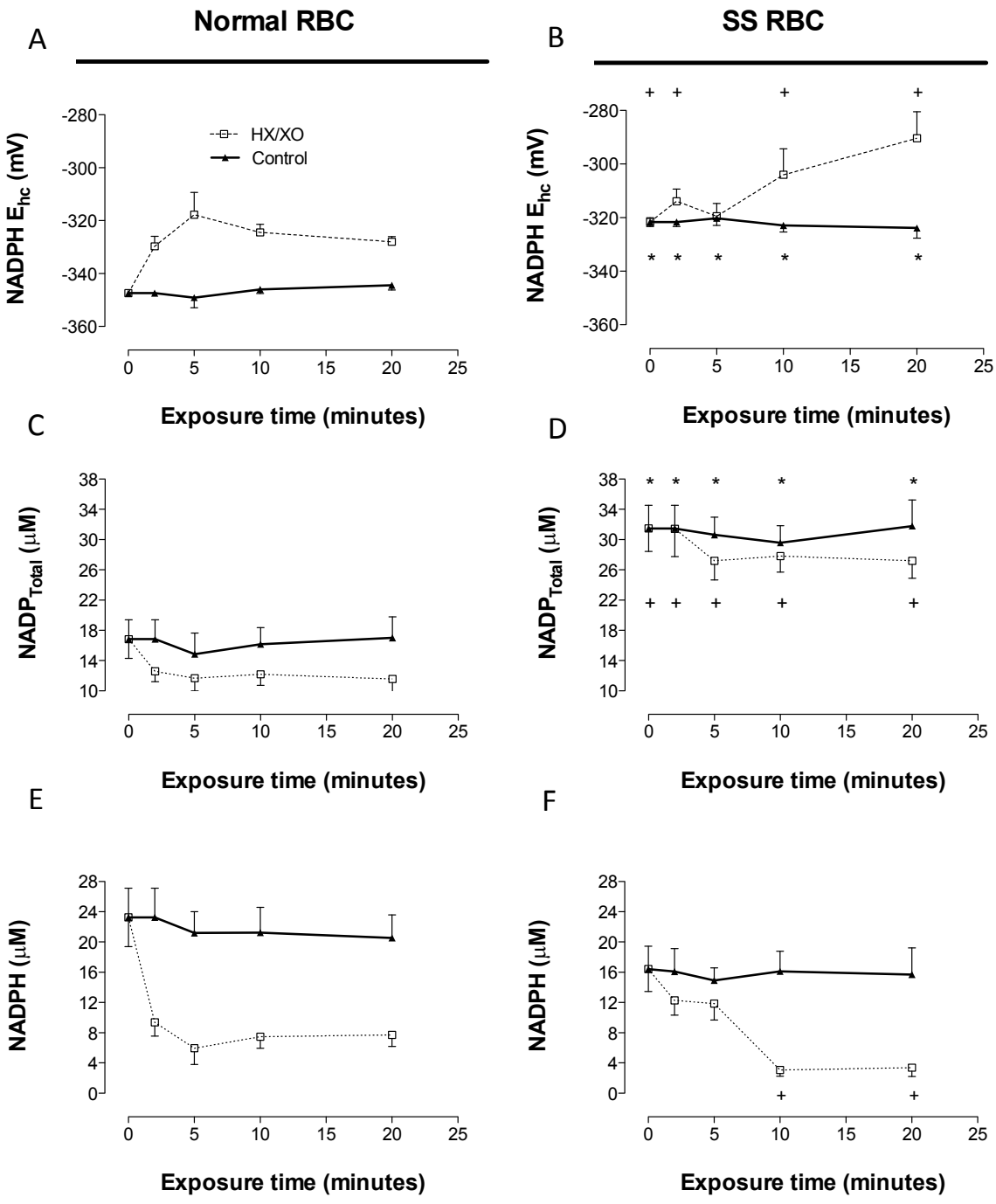
A
Normal RBC
B
SS RBC
HX/XO
Control
NADPH E_hc (mV)
-280
-300
-320
-340
-360
0
5
10
15
20
25
Exposure time (minutes)
C
D
NADP_Total (μM)
38
34
30
26
22
18
14
10
E
F
NADPH (μM)
28
24
20
16
12
8
4
0

FIGURE 3

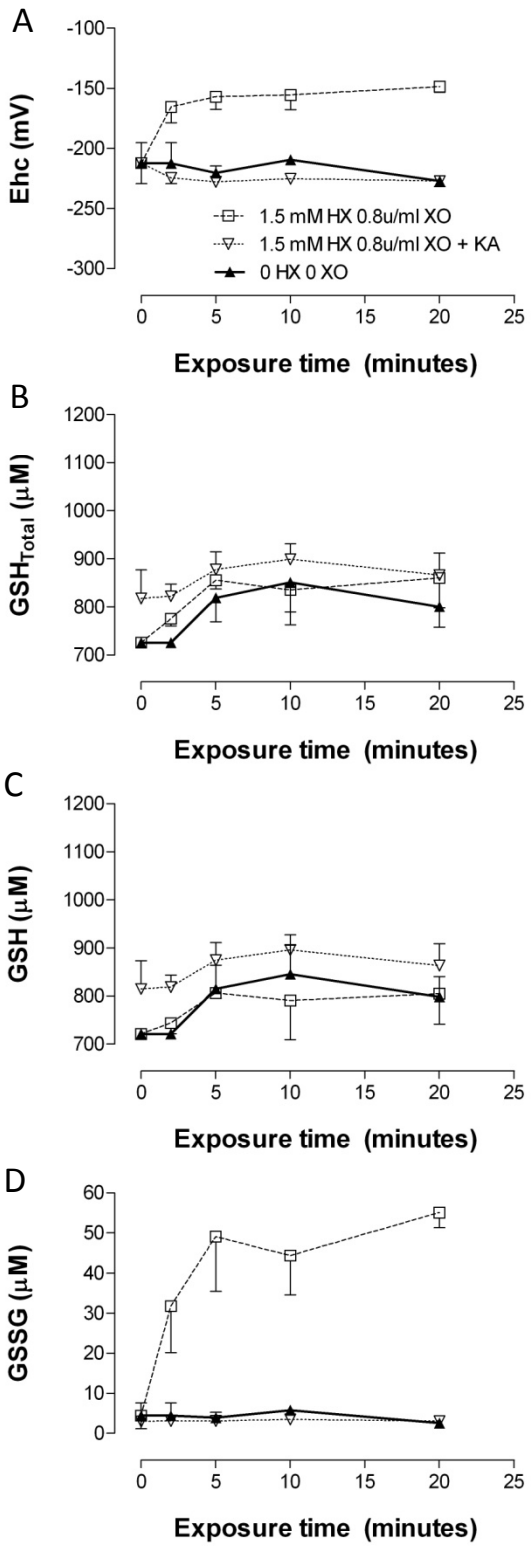
A
Ehc (mV)
-100
-150
-200
-250
-300
1.5 mM HX 0.8u/ml XO
1.5 mM HX 0.8u/ml XO + KA
0 HX 0 XO
0
5
10
15
20
25
Exposure time (minutes)
B
GSHTotal (µM)
1200
1100
1000
900
800
700
Exposure time (minutes)
C
GSH (µM)
Exposure time (minutes)
D
GSSG (µM)
60
50
40
30
20
10
0
Exposure time (minutes)

FIGURE 4

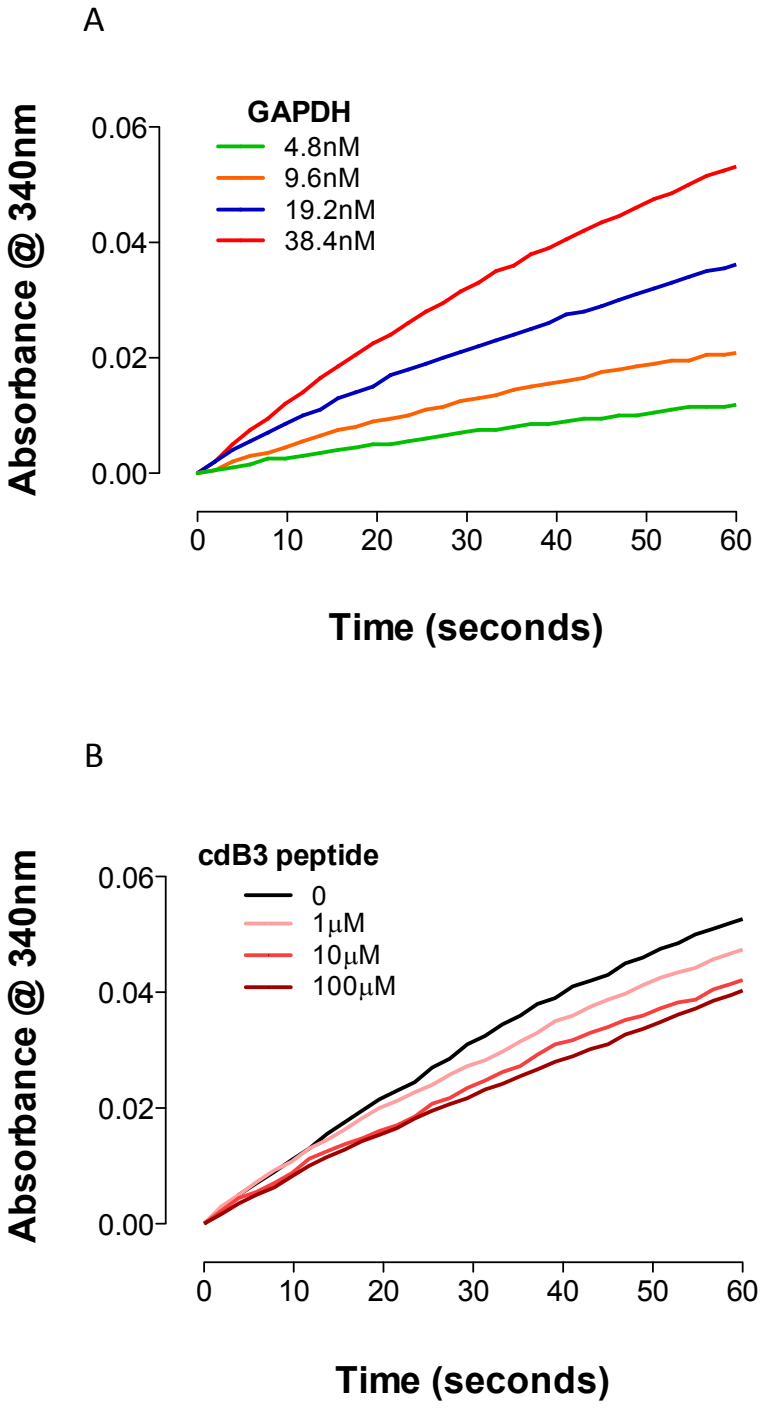
A
GAPDH
4.8nM
9.6nM
19.2nM
38.4nM
Absorbance @ 340nm
0.06
0.04
0.02
0.00
0
10
20
30
40
50
60
Time (seconds)
B
cdB3 peptide
0
1μM
10μM
100μM
Absorbance @ 340nm
0.06
0.04
0.02
0.00
0
10
20
30
40
50
60
Time (seconds)

FIGURE 5

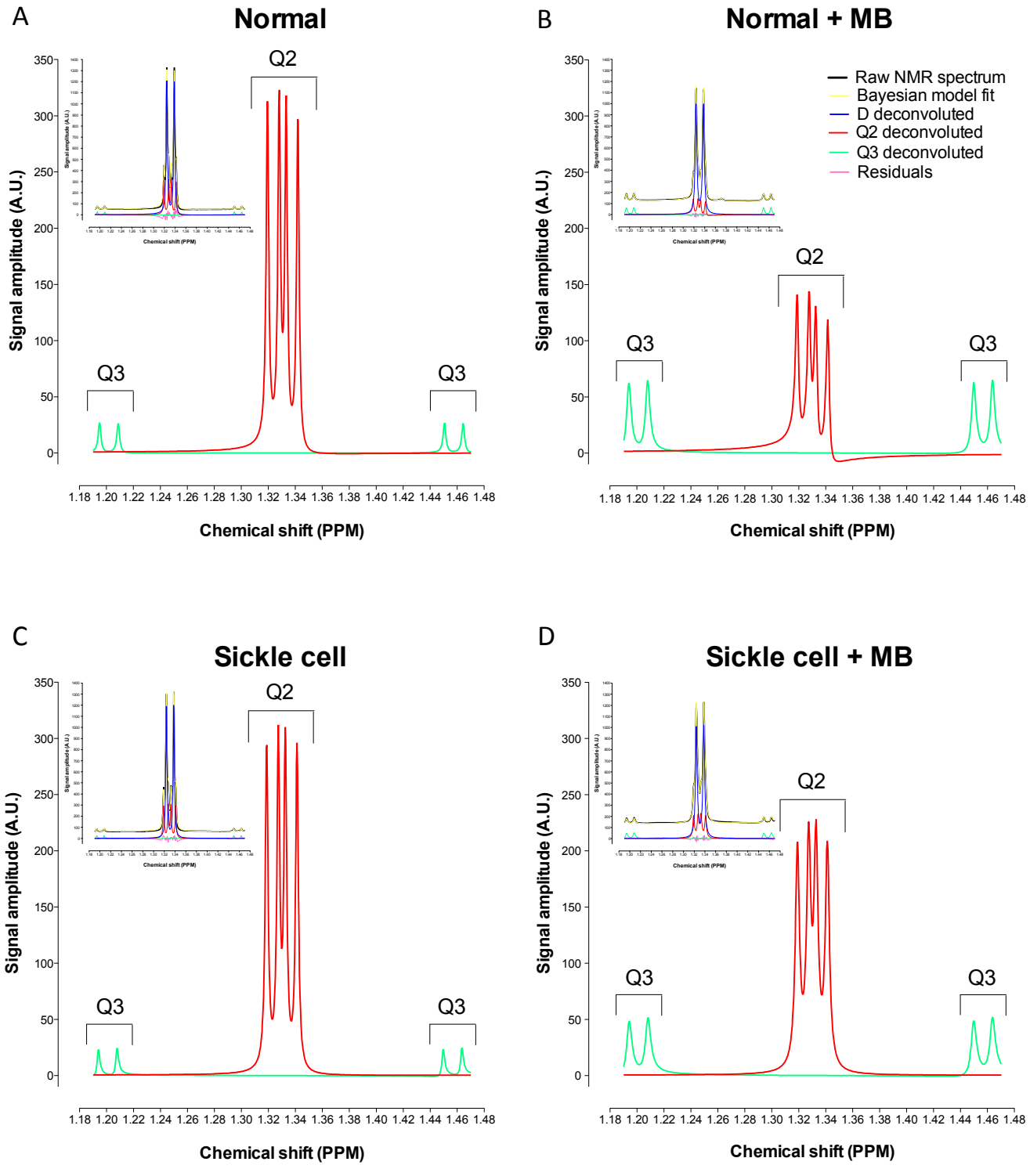
A
Normal
B
Normal + MB
C
Sickle cell
D
Sickle cell + MB
Q2
Q3
Q3
Raw NMR spectrum
Bayesian model fit
D deconvoluted
Q2 deconvoluted
Q3 deconvoluted
Residuals
Signal amplitude (A.U.)
Chemical shift (PPM)
0
50
100
150
200
250
300
350
1.18 1.20 1.22 1.24 1.26 1.28 1.30 1.32 1.34 1.36 1.38 1.40 1.42 1.44 1.46 1.48

FIGURE 6

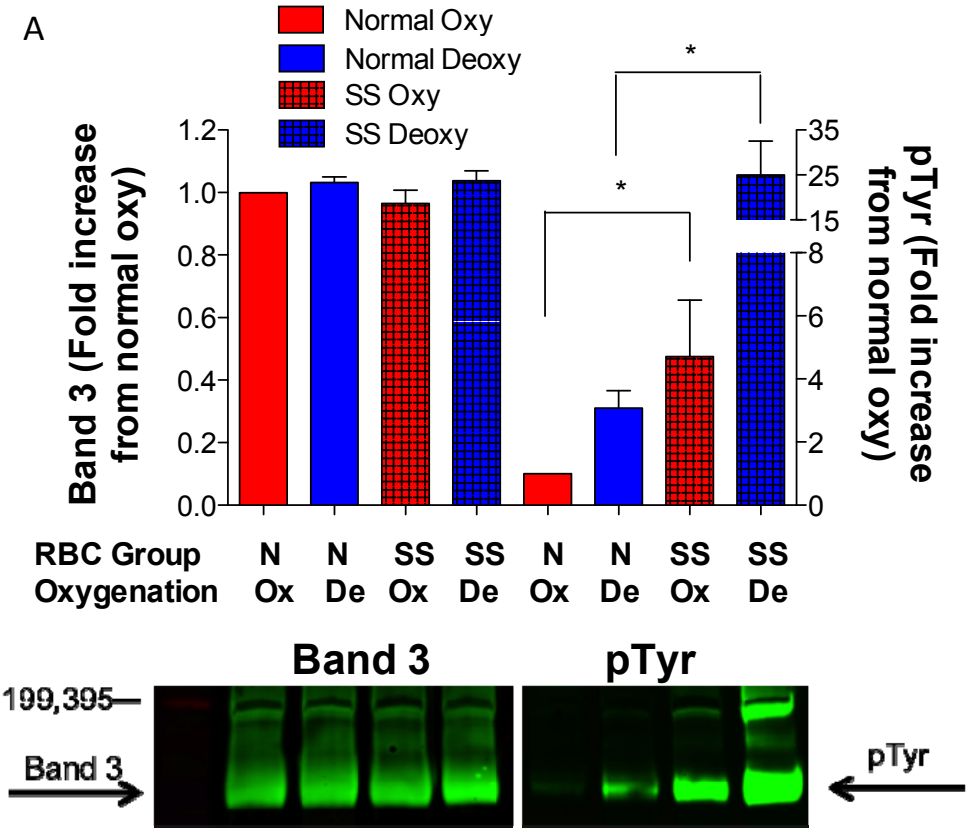
A
Normal Oxy
Normal Deoxy
SS Oxy
SS Deoxy
Band 3 (Fold increase from normal oxy)
pTyr (Fold increase from normal oxy)
RBC Group
Oxygenation
N Ox
N De
SS Ox
SS De
Band 3
pTyr
199,395
Band 3
pTyr

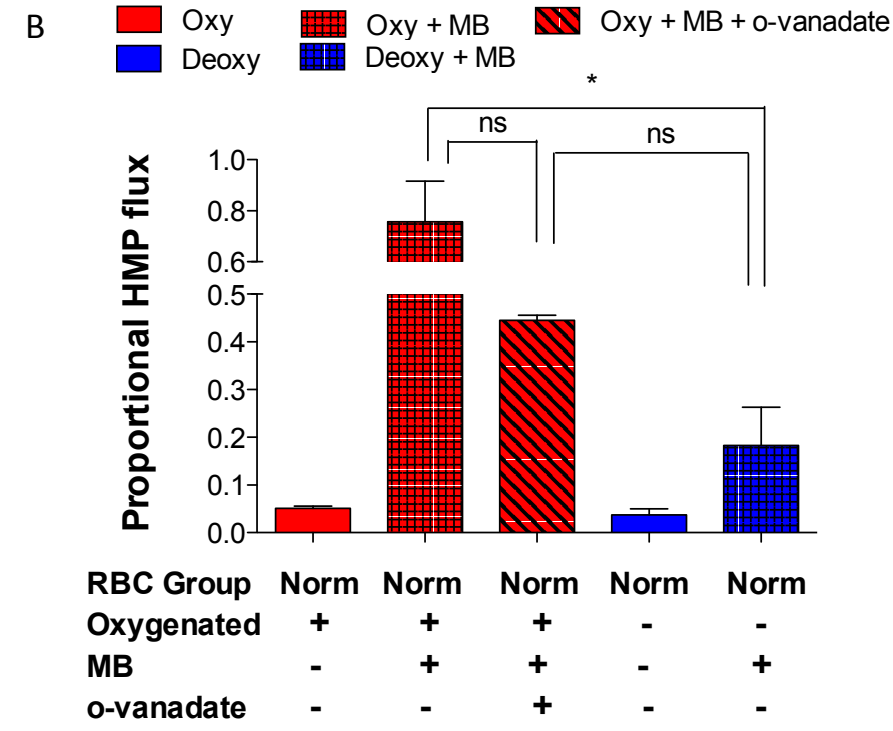
B
Oxy
Deoxy
Oxy + MB
Deoxy + MB
Oxy + MB + o-vanadate
Proportional HMP flux
ns
ns
RBC Group
Oxygenated
MB
o-vanadate
Norm

FIGURE 7

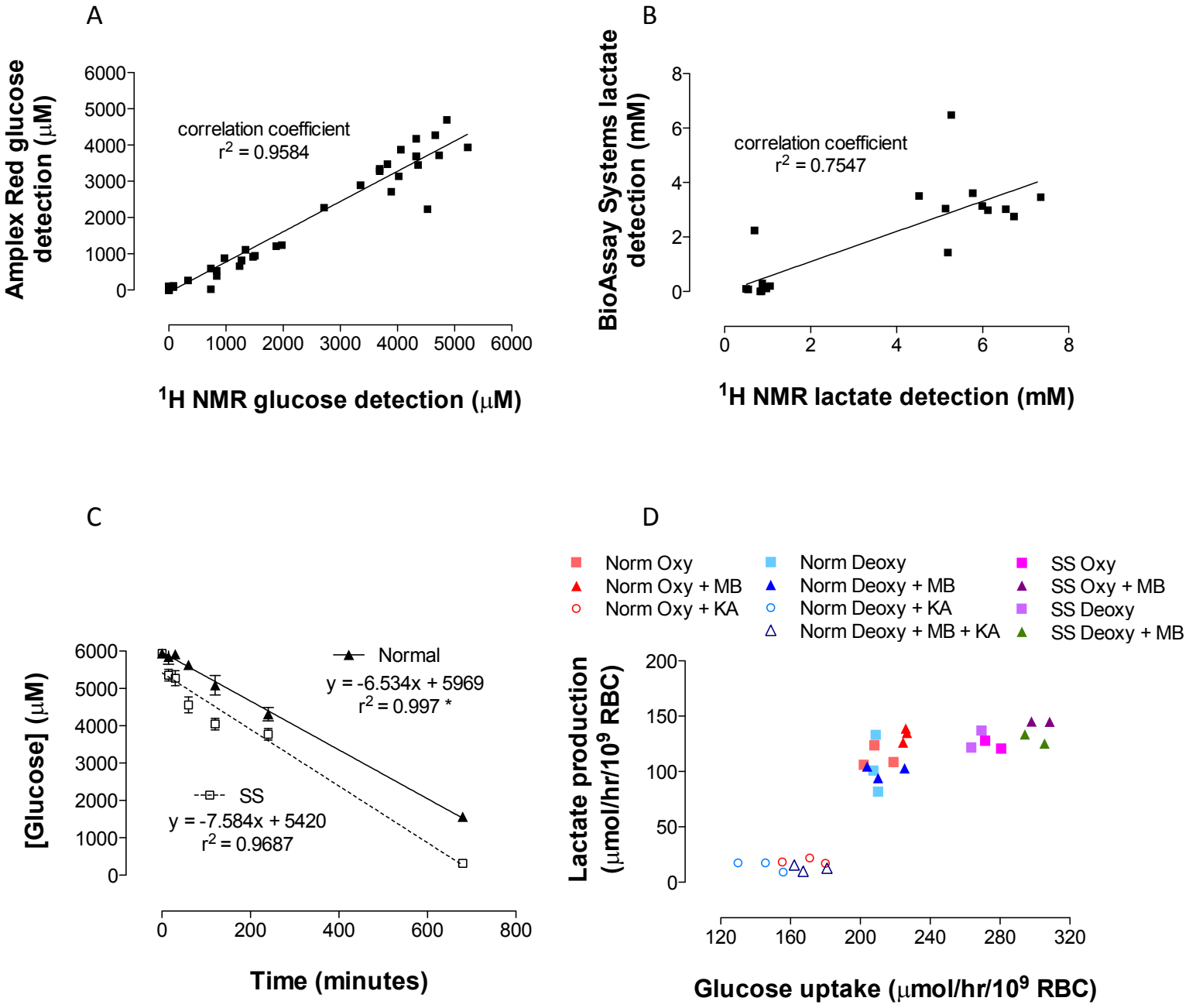
A
Amplex Red glucose detection (μM)
6000
5000
4000
3000
2000
1000
0
correlation coefficient
r2 = 0.9584
0
1000
2000
3000
4000
5000
6000
1H NMR glucose detection (μM)
B
BioAssay Systems lactate detection (mM)
8
6
4
2
0
correlation coefficient
r2 = 0.7547
0
2
4
6
8
1H NMR lactate detection (mM)
C
[Glucose] (μM)
6000
5000
4000
3000
2000
1000
0
Normal
y = -6.534x + 5969
r2 = 0.997 *
SS
y = -7.584x + 5420
r2 = 0.9687
0
200
400
600
800
Time (minutes)
D
Norm Oxy
Norm Oxy + MB
Norm Oxy + KA
Norm Deoxy
Norm Deoxy + MB
Norm Deoxy + KA
Norm Deoxy + MB + KA
SS Oxy
SS Oxy + MB
SS Deoxy
SS Deoxy + MB
Lactate production (μmol/hr/10^9 RBC)
200
150
100
50
0
120
160
200
240
280
320
Glucose uptake (μmol/hr/10^9 RBC)